ISSN 2072-5981
doi: 10.26907/mrsej

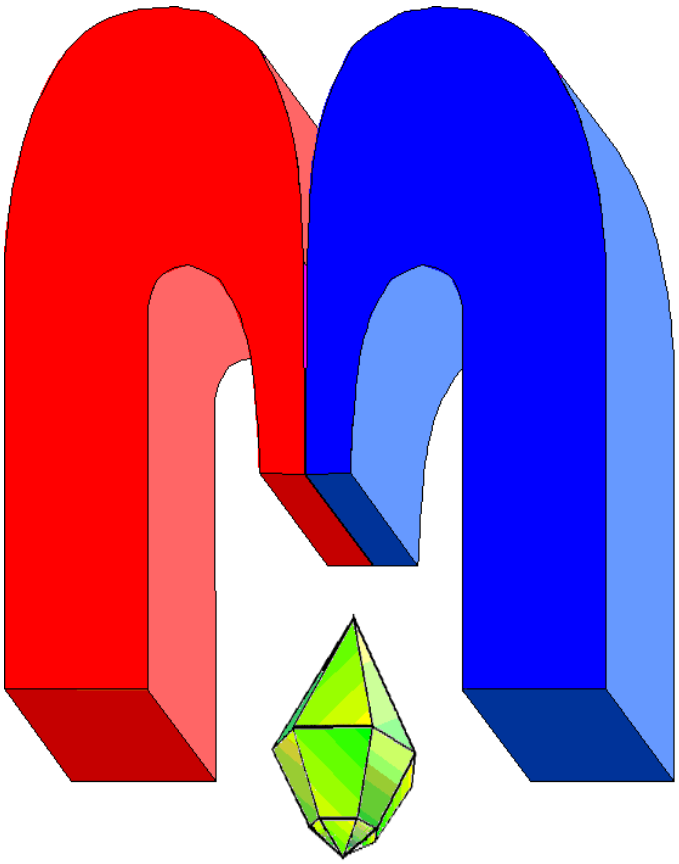

Magnetic Resonance in Solids

Electronic Journal

Volume ***26***
Issue ***1***
Article No ***24108***
1-6 pages
April, ***19***
2024
doi: **10.26907/mrsej-24108**

http://mrsej.kpfu.ru
https://mrsej.elpub.ru

Established and published by Kazan University*
Endorsed by International Society of Magnetic Resonance (ISMAR)
Registered by Russian Federation Committee on Press (#015140), August 2, 1996
First Issue appeared on July 25, 1997

"***Magnetic Resonance in Solids. Electronic Journal***" (**MRS*ej***) is a peer-reviewed, all electronic journal, publishing articles which meet the highest standards of scientific quality in the field of basic research of a magnetic resonance in solids and related phenomena.

Indexed and abstracted by
Web of Science (*ESCI*, Clarivate Analytics, from 2015), *Scopus* (Elsevier, from 2012), *RusIndexSC* (*eLibrary*, from 2006), *Google Scholar*, *DOAJ*, *ROAD*, *CyberLeninka* (from 2006), *SCImago Journal & Country Rank*, etc.

* Address: "Magnetic Resonance in Solids. Electronic Journal", Kazan Federal University; Kremlevskaya str., 18; Kazan 420008, Russia

† In Kazan University the Electron Paramagnetic Resonance (EPR) was discovered by Zavoisky E.K. in 1944.

Short cite this: *Magn. Reson. Solids* **26**, 24108 (2024) doi: 10.26907/mrsej-24108

Electronic and optical properties of planar MoS_2/WS_2 heterostructure†

E.P.Sharin

North-Eastern Federal University, Yakutsk 677000, Russia

**E-mail: ep.sharin@s-vfu.ru*

(Received March 14, 2024; accepted April 15, 2024; published April 19, 2024)

The electronic structure and optical properties of the MoS_2/WS_2 planar heterostructure are studied based on density functional theory. Compared with single-layer MoS_2 and WS_2, the MoS_2/WS_2 heterostructure has an indirect and very narrow band gap. In the visible region of the light spectrum, the maximum values of dielectric constant, refractive index and attenuation coefficient for MoS_2/WS_2 are shifted to the blue region of the spectrum.

PACS: 73.22.-f, 78.67.-n.

Keywords: density functional theory, MoS_2/WS_2 planar heterostructure, optical properties, permittivity, refractive index, damping factor, band structure.

1. Introduction

Advances in the synthesis of crystals of atomic thickness and experimental methods for determining various characteristics of such crystals have opened up the possibility of forming various heterostructures with new functional properties [1, 2]. Vertical and planar heterostructures (MoS_2/WS_2 and $MoSe_2/WSe_2$) were obtained by chemical vapor deposition of elements. In vertical heterostructures, atomic monolayers combine to form a van der Waals heterostructure, in which monolayers of several two-dimensional materials are stacked vertically layer by layer. In planar heterostructures, materials are combined along the layers and atoms interact with each other through strong covalent bonds. Vertical (van der Waals) heterostructures are interesting for flexible optoelectronic applications. Many distinctive properties and high-performance devices based on vertical heterostructures have been demonstrated and investigated [1, 3, 4]. Lateral heterojunctions can also lead to new and interesting physical phenomena and applications. For example, semiconductor monolayers of transition metal dichalcogenides (TMDs) can serve as building blocks for *p-n* junctions and other optoelectronic devices [5, 6]. However, fabricating 2D heterostructures with clean and sharp interfaces required to maintain optoelectronic properties due to interlayer or intralayer coupling remains challenging. These studies can be useful for applications in optoelectronics, sensoring and quantum information [7–12]. It should be noted that the tunable band gap, high carrier mobility, high optical absorption and atomically thin thickness make TMD a suitable material for photodetectors and play a crucial role in optoelectronic or electronic devices [13]. Monolayers of molybdenum dichalcogenide and tungsten dichalcogenide are direct-gap semiconductors with band gaps of about 1.8 and 2.05 eV, respectively. They have many excellent properties, such as high electron mobility, small size, and unique mechanical properties. By combining different two-dimensional materials together it is possible to create vertical and lateral artificial materials with amazing structural, physical and chemical properties. These unique physical and chemical properties make such heterojunctions even more important than the 2D material itself. Currently, modern experimental setups make it possible to synthesize both vertical and planar TMD heterostructures with different physical and chemical properties. Such heterostructures can change the internal electronic properties and

†This paper is dedicated to Professor Boris I. Kochelaev on the occasion of his 90th birthday.

improve optical absorption, demonstrating new design features. Due to limitations in experimental methods, the properties of such heterostructures have not been fully studied. Theoretical studies of the optical properties of heterostructures are still missing. The purpose of the presented work is the quantum mechanical calculation of the band structure, complex dielectric constant, refractive indices and attenuation of the planar MoS_2/WS_2 heterostructure.

2. Calculation method

All calculations were performed within the framework of density functional theory (DFT) using the pseudopotential approach in the Quantum Espresso package. The exchange-correlation potential is described by the generalized gradient approximation (GGA-PBE). The sampling of electronic states in the Brillouin zone is approximated by a set of special k points corresponding to the Monkhorst-Park grid ($12 \times 12 \times 1$) for MoS_2 and WS_2 monolayers, as well as the Monkhorst-Park grid ($9 \times 9 \times 1$) for the proposed planar MoS_2/WS_2 heterostructure. To minimize interactions between two cells, this supercell heterostructure is separated by a 20 Å vacuum buffer space in the z direction, which is perpendicular to the plane of the heterolayer. The equilibrium structure is determined by minimizing the total energy with respect to the lattice parameters, and the internal parameters of the structure are optimized using the Gelman–Feynman force. The minimization process was carried out until the residual forces on the atoms fell below 0.003 eV/Å.

3. Resuts and Discussion

MoS_2 and WS_2 monolayers form hexagonal lattices. The lattice constants of MoS_2 and WS_2 monolayers are $a_{MoS_2} = 3.16$ Å and $a_{WS_2} = 3.15$ Å respectively. The mismatch between the crystal lattices of both structures is minimal, so they are ideal for forming a planar heterostructure. Planar heterostructures are formed from two-dimensional materials by combining them along layers. In this work, we consider a heterostructure whose supercell size is 3×3. Figure 1 shows possible crystal structures of the MoS_2/WS_2 heterostructure with a 3×3 supercell. According to the classification, these structures are designated as $(MoS_2)_2/(WS_2)_1$ and $(MoS_2)_1/(WS_2)_2$, respectively [13]. We carry out all calculations for the $(MoS_2)_2/(WS_2)_1$ heterostructure.

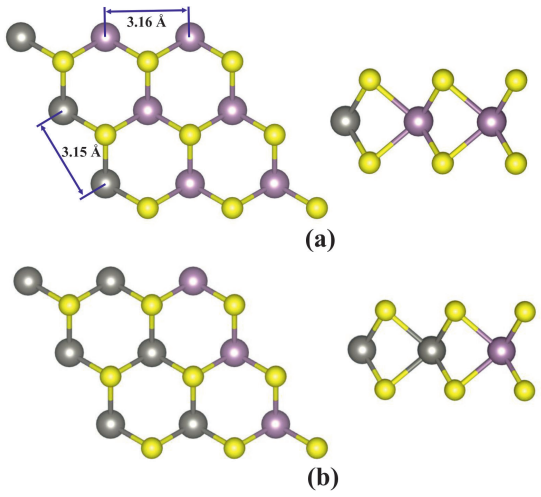

Figure 1. Possible crystal structures of planar MoS_2/WS_2 heterostructure with a 3×3 supercell: (a) – $(MoS_2)_2/(WS_2)_1$ and (b) – $(MoS_2)_1/(WS_2)_2$.

Figure 2 shows the calculated electronic band structure of the planar MoS_2/WS_2 heterostruc-

ture. MoS_2 and WS_2 monolayers are direct gap semiconductors with band gaps of 1.8 eV and 2.0 eV, respectively. It can be seen that the planar heterostructure MoS_2/WS_2 is an indirect gap semiconductor with a band gap of approximately 0.59 eV. For a comparative study of the optical properties of MoS_2, WS_2 monolayers and the planar MoS_2/WS_2 heterostructure, we proceed from calculations of complex dielectric constants [14]. Knowing these values, we calculated the refractive and attenuation coefficients for these systems. Figure 3 shows the real (a) and imag-

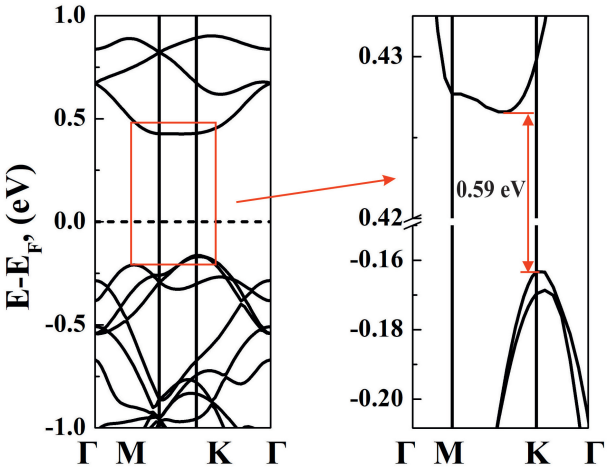

Figure 2. Band structure of the MoS_2/WS_2.

inary (b) parts of the complex dielectric constant. The dotted lines mark the region belonging to the visible region of the light spectrum. This region lies in the range of $1.8 \div 3.1$ eV. As is known, the real part of the dielectric constant $\varepsilon_1(\omega)$ is included in the expression for electrical induction and determines the polarization of the medium. It is responsible for storing energy in the environment. In the visible region of the light spectrum, the real part of the dielectric constant is greatest for the WS_2 monolayer, followed by the WS_2 monolayer and then the flat MoS_2/WS_2 heterostructure. This suggests that this system can store less energy than the other two systems. In this spectral region, the maximum values of $\varepsilon_1(\omega)$ for the MoS_2 and MoS_2/WS_2 systems are shifted to the blue region of the spectrum, and the maximum $\varepsilon_1(\omega)$ for the WS_2 system is shifted to the red region. Imaginary part of the complex dielectric constant $\varepsilon_2(\omega)$ is re-

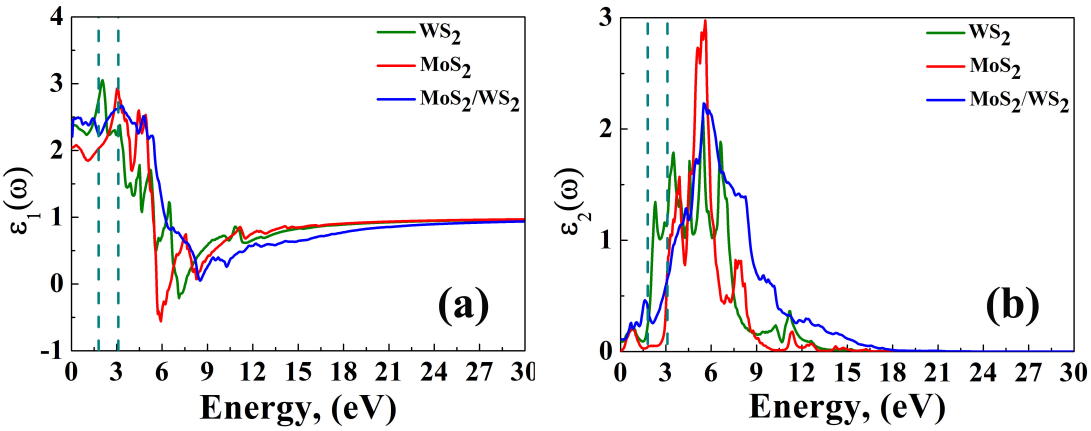

Figure 3. The complex dielectric constants of monolayer WS_2, monolayer MoS_2 and MoS_2/WS_2 systems. (a,b) represent the real part and the imaginary part of the dielectric constant, respectively.

lated to the conduction current density and characterizes the energy loss of the electromagnetic

field in the medium. The discussion above concerning the real part of the dielectric constant are also true for the imaginary part $\varepsilon_2(\omega)$. When an electromagnetic wave passes through any medium, some part of the wave will be absorbed. The complex refractive index is defined as [15]

$$n^* = n + ik, \tag{1}$$

where n^* is the complex refractive index, n is the real part refractive index, k is the attenuation index. The refractive and attenuation indices are related to $\varepsilon_1(\omega)$ and $\varepsilon_2(\omega)$ by the following relations [15]

$$n = \frac{1}{\sqrt{2}}\sqrt{\varepsilon_1 + \sqrt{{\varepsilon_1}^2 + {\varepsilon_2}^2}}, \quad k = \frac{2n}{\varepsilon_2}. \tag{2}$$

Using these formulas, we determine the refractive and attenuation indices of the electromagnetic wave depending on the photon energy. Figures 4 and 5 show the calculated dependences of the refractive and attenuation indices for all three systems on the photon energy. For the WS_2 system in the visible part of the spectrum, the maximum value of the refractive index lies in the region of low energy values (in the red region), while for the MoS_2/WS_2 and MoS_2 systems the maximum values lie in the region of high energy values (in the blue region) (see Fig. 4).

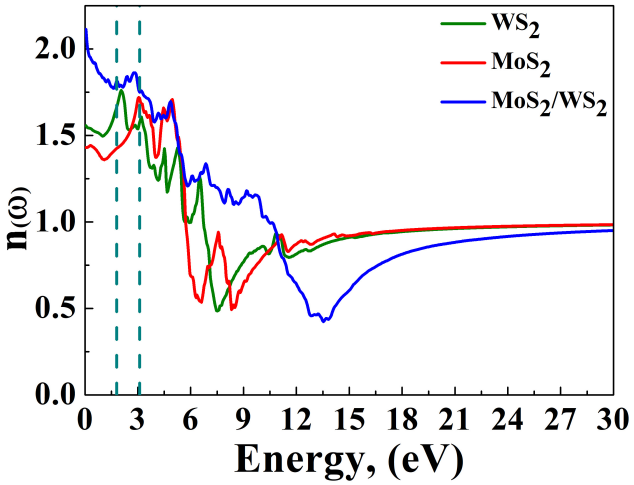

Figure 4. Dependence of the real refractive index on photon energy for three systems.

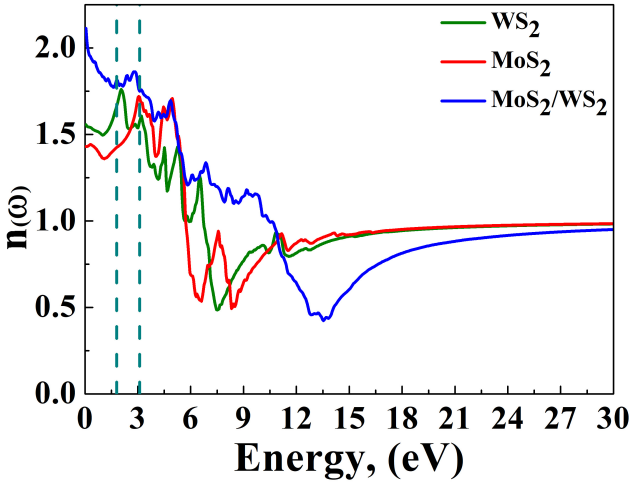

Figure 5. The attenuation index $k(\omega)$ of monolayers MoS_2, WS_2 and MoS_2/WS_2 heterostructure.

In the visible light region of the spectrum, the MoS_2 monolayer is of greatest importance, then the MoS_2/WS_2 heterostructure and then the MoS_2 system. For the attenuation coefficient, in general, the same picture is observed as for the refractive index. The exception is that the maximum values for all three systems lie in the ultraviolet region of the spectrum.

4. Summary

In this work we investigate the electronic and optical properties of a planar MoS_2/WS_2 heterostructure from ab initio calculations. Based on the density functional theory method, the band structure, complex dielectric constant, real refractive indices and attenuation indices of single-layer MoS_2, WS_2 structures and planar MoS_2/WS_2 heterostructure are calculated. It should be noted that during the formation of a planar heterostructure, the nature of the electronic band structure changes. The heterostructure becomes an indirect gap semiconductor with a band gap of 0.59 eV. In general, in the visible light region the optical properties (dielectric constant, real refractive index, and attenuation index) of the $(MoS_2)_2/(WS_2)_1$ heterostructure are inferior to the WS_2 monolayer. For the $(MoS_2)_2/(WS_2)_1$ system, the highest values of dielectric constant, real refractive index and attenuation index lie in the red region. The results obtained can be used to interpret experimental data.

References

1. Grigorieva I. V., Geim A. K., *Nature* **499**, 419 (2013).

2. Xia F., Wang H., Xiao D., Dubey M., Ramasubramaniam A., *Nature Photonics* **8**, 899 (2014).

3. Georgiou T., Jalil R., Belle B. D., Britnell L., Gorbachev R. V., Morozov S. V., Kim Y.-J., Gholinia A., Haigh S. J., Makarovsky O., Eaves L., Ponomarenko L. A., Geim A. K., Novoselov K. S., Mishchenko A., *Nature* **8**, 100 (2013).

4. Yu W. J., Liu Y., Zhou H., Yin A., Li Z., Huang Y., Duan X., *Nature Nanotechnology* **8**, 951 (2013).

5. Pospischil A., Furchi M. M., Mueller T., *Nature Nanotechnology* **9**, 257 (2014).

6. Baugher B. W., Churchill H. O., Yang Y., Jarillo-Herrero P., *Nature Nanotechnology* **9**, 262 (2014).

7. Xu H., Han X., Dai X., Liu W., Wu J., Zhu J., Kim D., Zou G., Sablon K. A., A. Sergeev Z. G., Liu H., *Nature Nanotechnology* **30**, 1706561 (2018).

8. Du W., Yu P., Zhu J., Li C., Xu H., Zou J., Wu C., Wen Q., Ji H., Liu T., Li Y., Zou G., Wu J., Wang Z. M., *Nanotechnology* **31**, 225201 (2020).

9. Du W., Li C., Sun J., Xu H., Yu P., Ren A., Wu J., Wang Z., *Appl. Magn. Reson.* **14**, 202070066 (2020).

10. He Y.-M., Clark G., Schaibley J. R., He Y., Chen M.-C., Wei Y.-J., Ding X., Zhang Q., W. Yao C.-Y. L., X. Xu, Pan J.-W., *Nature Nanotechnology* **4**, 219 (2022).

11. Turunen M., Brotons-Gisbert M., Dai Y., Wang Y., Scerri E., Bonato C., K. D. Jons Z. S., Gerardot B. D., *Nature Reviews Physics* **178**, 42 (2003).

12. Shen P. C., *Large-area CVD growth of two-dimensional transition metal dichalcogenides and monolayer MoS2 and WS2 metal-oxide-semiconductor field-effect transistors*, Ph.D. thesis, Massachusetts Institute of Technology (2017).

13. Wang X., Lu Y., Zhang J., Zhang S., Chen T., Ou Q., Huang J., *Small* **17**, 2005491 (2021).

14. Tang Y., Li H., Maoa X., Xie J., Lee J. Y., Fu A., *RSC advances* **9**, 34986 (2019).

15. Shashikant R. S., *Electrical, electronic and optical properties of $MoSe_2$ and WSe_2*, Ph.D. thesis, New Jersey Institute of Technology (2017).